Materials Research Proceedings **32** (2023) 55-63 https://doi.org/10.21741/9781644902615-5

An investigation of forming of Ti-6Al-4V at lower temperatures

Hosam Elrakayby[1,a,*], Diego Gonzalez[1,b], Paranjayee Mandal[1,2,c] and Paul Blackwell[1,d]

[1]Advanced Forming Research Centre, University of Strathclyde, 85 Inchinnan Drive, Inchinnan, Renfrewshire PA4 9LJ, Scotland

[2]Now at BorgWarner Inc., Courteney Road, Gillingham ME8 0RU, England

[a]hosam.elrakayby@strath.ac.uk, [b]diego.gonzalez@strath.ac.uk, [c]pmandal@borgwarner.com, [d]paul.blackwell@strath.ac.uk

Keywords: Superplastic Forming, Titanium, Ti-6Al-4V, Alpha Case

Abstract. Forming components of titanium alloys via superplastic forming at elevated temperatures while being exposed to oxygen leads to surface oxidation. The hard oxide layer formed on the surface of components is referred to as the alpha case. This alpha case layer requires post-form processing to remove it, thus increasing overall manufacturing costs and times. Superplastic forming at lower temperatures can significantly reduce the formation of the alpha case and has other benefits, such as life extension of tooling and less energy consumption. This paper shows the work done in terms of forming non-commercial components at temperatures significantly lower than the traditional ones, proving that forming at those temperatures is readily achievable. Forming pressures and tonnage need to be readjusted because of the increase in the flow stresses of the material. This paper also illustrates the implementation of a microstructural-based model to predict the hot forming behaviour of commercial titanium alloy Ti-6Al-4V (Ti64) during forming at 800°C. The material model is implemented into a commercial finite element software, Abaqus, and PAM-STAMP to obtain the optimal pressure cycle to form a non-commercial research component at 800 °C with a view to minimizing alpha case formation.

1. Introduction

Titanium alloys in general, and commercial Ti64 in particular, are optimal candidates for aerospace sector applications due their high strength-to-weight ratio, corrosion resistance and fatigue strength [1]. For a long time, the aerospace sector has been forming Ti64 through SPF to obtain near-net complex shapes without springback and residual stresses. Typically, Ti64 is superplastically formed at optimum SPF conditions, with temperatures close to 900 °C [2–4]. The exposure of titanium alloys to air/Argon at a high temperature (>650°C) during the SPF process frequently results in surface oxidation [5]. This oxygen-enriched layer, referred as alpha case, is hard, brittle and very abrasive in nature, thus producing excessive tool wear. Alpha case can be removed by machining or chemical etching, which increases the costs and the times of manufacturing (and etching makes use of environmentally harmful chemicals).

Superplastic forming (SPF) manufacturers in the Aerospace industry pursue lower forming temperatures due to the associated benefits in terms of alpha case thickness reduction, tooling and heating element life extension, less energy consumption together with the possibility of using cheaper platen and die materials [6]. Previous work [7,8] was done to obtain ultra fine grained Ti64 through severe plastic deformation to improve the superplasticity of Ti64 material at lower temperatures.

This work investigates the possibility of forming Ti64 superplastically at 800 °C, well below the optimum conditions. Tensile testing has been performed at 800 °C (ASTM E2448) and subsequent microstructural analysis of the samples has been fed into a microstructural-based

Materials Research Proceedings **32** (2023) 55-63 https://doi.org/10.21741/9781644902615-5

material model. This material model is then implemented into a commercial finite element software Abaqus and PAM-STAMP to obtain the optimal pressure cycle to form a non-commercial component.

2. Experimental Methodology

TIMETAL® 6-4 sheet (Ti64) material (produced by TIMET) with a bimodal microstructure was used in this work. The average grain size and primary α-phase volume fraction were ~2.3 μm and 90%, respectively.

Mechanical Characterization. A series of strain rate jump and interrupted tensile tests were conducted to identify the optimal forming conditions for Ti64 material within the temperature range under consideration. Strain rate jump tensile tests were conducted at temperatures of 750, 775, 800 and 825 °C and strain rates of 10^{-4} s^{-1}, $2x10^{-4}$ s^{-1} and $5x10^{-4}$ s^{-1}. Once the optimum forming window was defined, a small number of interrupted tests at a predefined strain (0.7) and temperature were carried out. One set of the interrupted tests were followed by air-cooling outside the furnace mainly for studying the alpha case formed and the other set was water-quenched to study the grain size after testing. To mimic the forming conditions during forming components in a press, all tensile tests samples were coated with boron nitride (BN) and tested in an air environment. All tensile samples were cut by wire electro-discharge machining (EDM) with geometries following the ASTM E2448 standard.

Microstructural Analysis. The as-received and tested interrupted tensile samples were characterised for microstructure using a FEI 650 Quanta SEM to assess the presence of voids and/or cavities, alpha-beta volume fraction and grain size analysis. A Leica DM1200M optical microscope was used to image alpha case formed on interrupted tensile test samples after etching with 100 mL water, 25 mL ethanol and 2 g ammonium bifluoride. Table 1 summarises the testing conditions of these investigated samples.

Table 1 Conditions of samples for grain size measurements

Sample	Measurement	Temperature (°C)	Interrupted True Strain	Strain rate (s^{-1})	Soak Time	Coating	Cooling
C1	After Deformation (tensile test)	800	0.3	$1x10^{-4}$	50 min before starting tensile test (dwell time)	Boron Nitride	Water-Quenched
C2			0.7				
C3			0.3	$5x10^{-4}$			
C4			0.7				
C5	Before Deformation (heat treatment only)	800	N/A	N/A	50	Boron Nitride	Water-Quenched
C6					100		
C7					165		
C8					50		Air-Cooling
C9					100		
C10					165		

3. Finite Element Analysis

Constitutive Equations of the Material Model. For numerical modelling of the SPF process, a microstructural-based model was used to represent the material behaviour. Eq. 1 was used to model the grain size evolution during the forming process and the visco-plastic response of the material was expressed by a power-law based model in Eq. 2. [3,9–11]

$$\dot{d} = \dot{d}_{static} + \dot{d}_{dynamic} = \frac{\rho}{d^{\mu_1}} + \frac{\phi}{d^{\mu_2}}\dot{\varepsilon} \quad (1)$$

Where ρ, μ_1, φ and μ_2 are temperature-dependent material parameters. $\dot{\varepsilon}$ is the strain rate.

$$\dot{\varepsilon} = A\frac{\sigma^n}{d^p} \quad (2)$$

Where A, n and p are temperature-dependent material parameters.

Modelling of Microstructural and Mechanical Behaviour. The modelling of the Ti64 response during the high temperature tensile tests has been carried out by capturing numerically the grain size evolution at different testing conditions by obtaining the parameters of Eq. 1. Also, the flow curves of the tensile tests were fitted numerically by using Eq. 2 to optimise the parameters.
Modelling the SPF Process for a Research Demonstrator. The material model developed was used to obtain the pressure cycles to form a non-commercial research demonstrator. Numerical simulations were carried out by implementing the constitutive equations into Abaqus software via the CREEP subroutine. Also, numerical simulations were carried out in PAM-STAMP software using the built-in material data base. The purpose of having simulations in both software platforms was to compare the pressure cycles obtained, as each software platform is using different algorithms in controlling the strain rate in the formed material. Modelling was completed at different target strain rates of $1x10^{-3}$ and $5x10^{-4}$ s^{-1} to obtain the pressure cycles with limiting maximum pressure to 30 bar and 60 bar.

4. Forming Trials of Research Demonstrator

An ACB 200T press was used to complete the forming trials. Ti64 sheet material was cut into size of (500 x 500 x 1.2) mm then was sprayed by Boron Nitride. The press was heated to the target temperature then the sheet is loaded into the press and held for 15 min to stabilise the temperature in the press and confirm that the sheet reached the target temperature. Once the sheet reached the target temperature, the gas pressure was supplied based on the pressure curve obtained from the simulation.

After the forming cycle was completed, the pressure was released from the press over 5~10 min before unloading the part from the press.

5.Results and Discussion

Fig. 1 summarizes the flow curves obtained for the different test conditions and Fig. 2 summarises the calculated m-values for each test condition. It can be observed from the flow curves, that flow stress decreases with increasing the temperature and decreasing strain rates. Also, hardening behaviour was noted at the higher temperature (800 °C) and slower strain rates of $1x10^{-4}$ and $2x10^{-4}$ s^{-1}. while softening behaviour was observed at lower temperatures (750 and 775 °C) and highest strain rate; $5x10^{-4}$ s^{-1}. The m-values for the lower temperatures (750 and 775°C) are around 0.45 at different strain rates and true strains conditions. By increasing the temperature to 800 °C, the m-values increased to be around 0.5 at different strain rates and true strains. Even at this temperature and at lowest strain rate, the m-value was around 0.6. At 825 °C, m-values decreased to be around 0.47. Based on these results, 800 °C was selected to be the optimal condition for investigating the formability of Ti64 further through interrupted tensile tests.

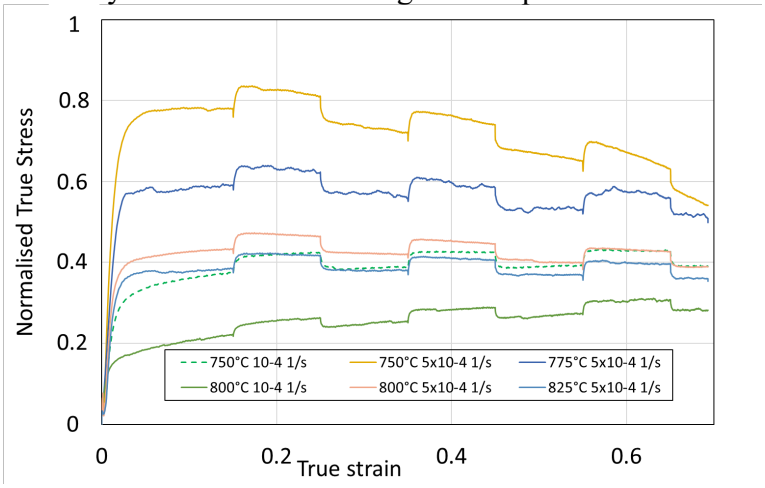

Fig. 1 Flow curves from jump tests

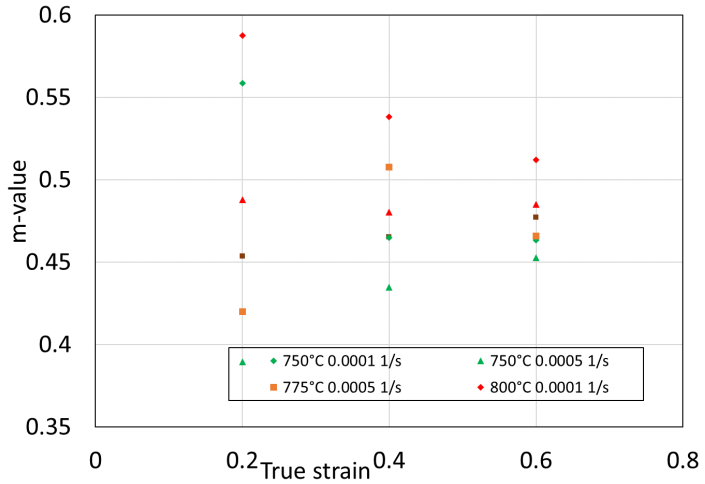

Fig. 2 m-values calculated from jump tests

Fig. 3 shows the flow curves obtained from the interrupted tensile tests. For the air-cooling condition a test was conducted at 900 °C to compare the alpha case generated at different temperatures. The flow curves at 800 °C agrees well with those obtained from the jump tests. Hardening behaviour can be noticed at lower strain rates, while curves are flattened at higher strain rates.

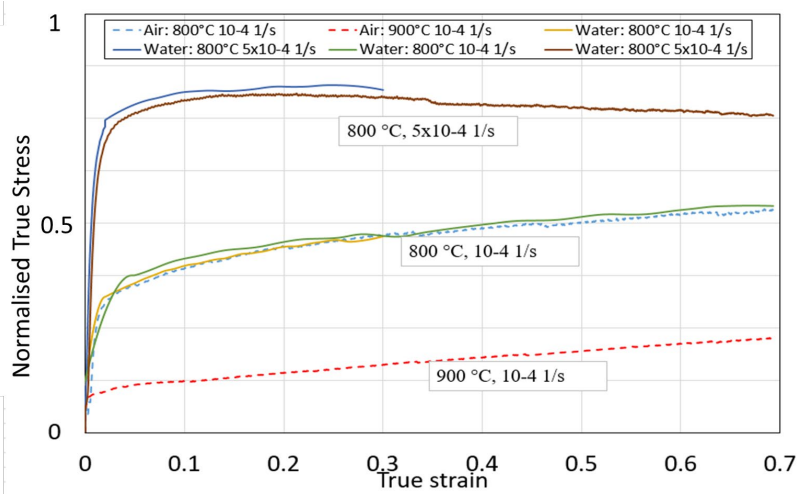

Fig. 3 Flow curves from interrupted tensile tests

Fig. 4 shows SEM images of different samples and Fig. 5 shows the average grain size and aspect ratio measured before and after the deformation at 800 °C. The as-received material has an average grain size for the alpha phase around 2.32 µm. The aspect ratio was measured at 1.87 and almost 95% alpha phase was observed as globular in shape. No grains were observed larger than 10 µm. Heat-treated samples without any deformation at 800°C show an average grain size of ~2.21 – 2.61 µm after water-quenching and ~2.09 – 2.57 µm after air-cooling. The aspect ratio was found to be in the range of ~1.71 – 1.79. Overall, no noticeable change is observed in the grain size after heat-treatment although the grains tended to globularise in all cases.

Deformed tensile samples tested at 800 °C followed by water-quenching showed an average grain size of ~2.33 – 3.05 µm, with an aspect ratio of 1.42 – 1.65 depending on the strain level and strain rate used. The typical microstructure contained fewer alpha clusters as compared to the as-received and heat-treated samples, rather, individual grain growth was observed, which led to a higher average grain size particularly for the slower strain rates. The average grain size was ~3 µm

for the lower strain rate, which then decreased to ~2.33 – 2.58 μm for the faster strain rate. With slower strain rates, the grains receive sufficient time and energy to grow.

Fig. 6 shows optical images of alpha case formed on interrupted tensile test sample (strain rate of $1x10^{-4}$ s^{-1} and 0.7 true strain) at 800 °C and 900 °C. Sample tested at 800 °C and 900 °C revealed alpha case formation with thickness ranges 4 - 18 μm and 7 - 20 μm, respectively.

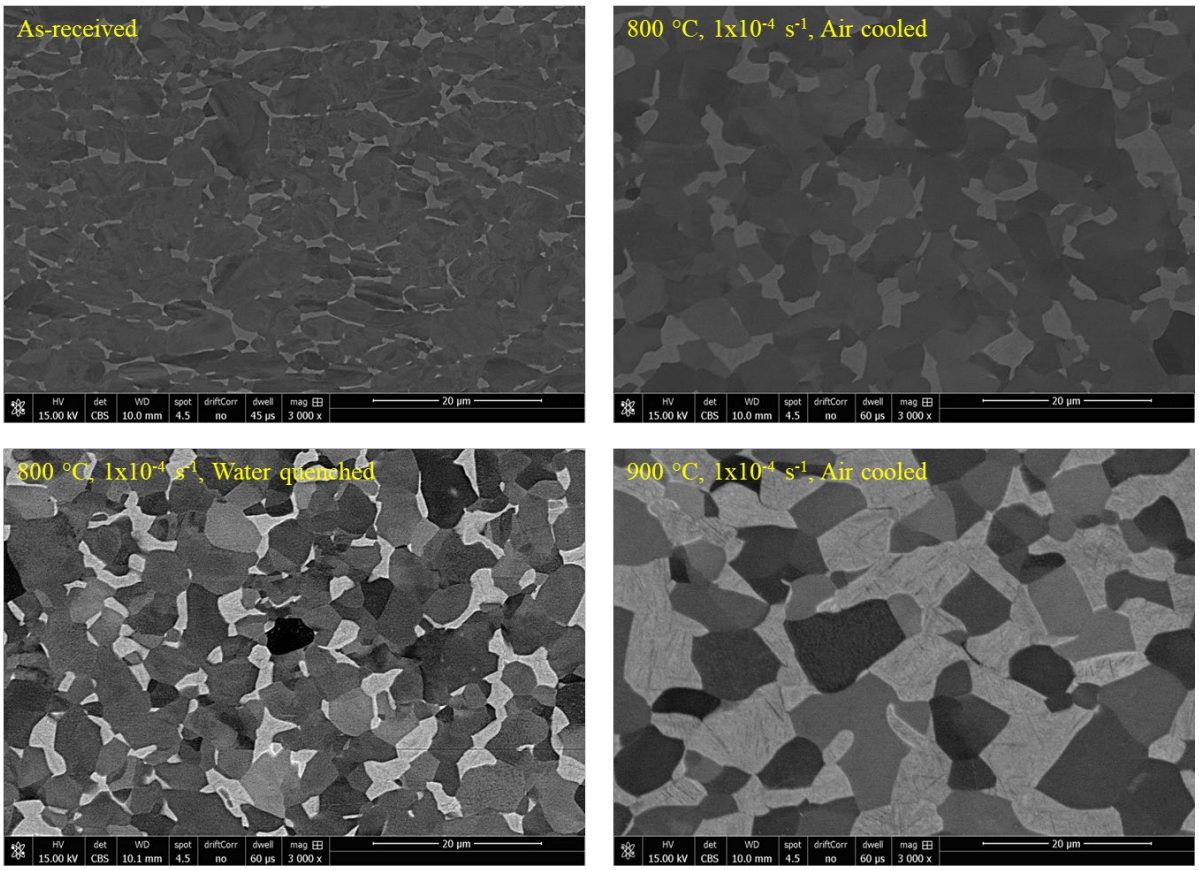

Fig. 4 SEM of different samples

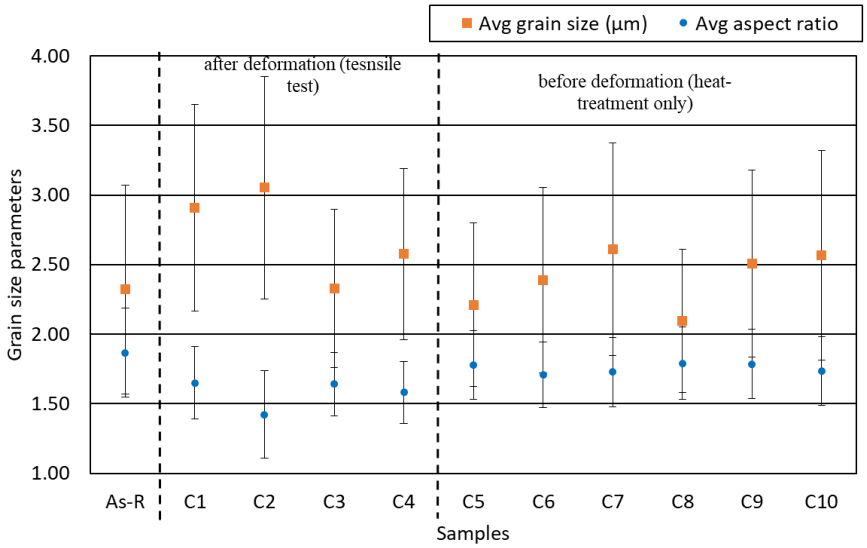

Fig. 5 Average grain size and aspect ratio measured before and after the deformation at 800 °C

Materials Research Proceedings **32** (2023) 55-63 https://doi.org/10.21741/9781644902615-5

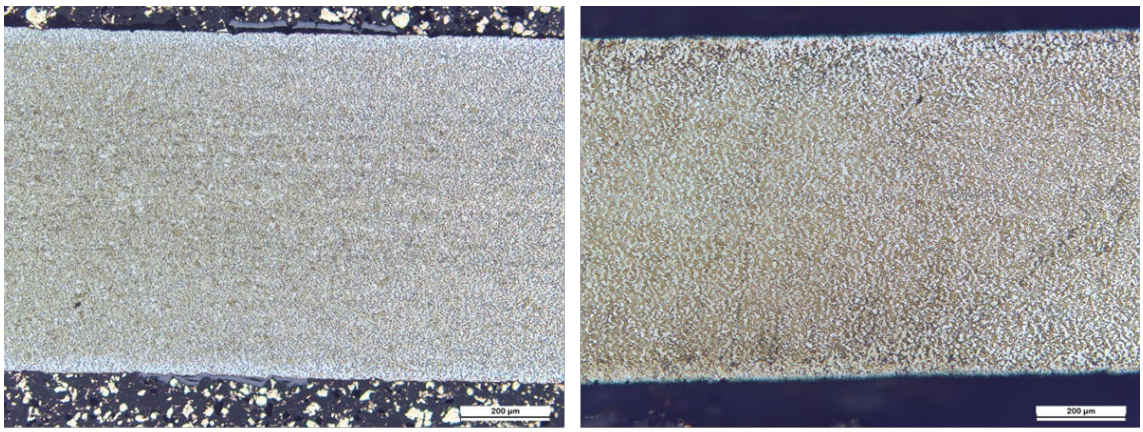

(a) 800 °C, 1x10^{-4} s^{-1}, Air cooled
Alpha case thickness: 4 – 18 µm

(b) 900 °C, 1x10^{-4} s^{-1}, Air cooled
Alpha case thickness: 7 – 20 µm

Fig. 6 Optical microscopy for alpha case measurement at (a) 800 and (b) 900 °C

Table 2 Material model parameters

Parameter	μ_1	μ_2	n	p
Value	0.86	2.13	3	1.5

Fig. 7 shows the fitting for the grain size data with time at 800 °C and strain rates 1x10^{-4}, 5x10^{-5} s^{-1} and also in the static condition with no deformation. The model parameters obtained are summarised in Table 2. Fig. 8 shows the fitting for the flow data at 800 °C and strain rates 1x10^{-4} and 5x10^{-5} s^{-1}. The model parameters obtained are summarised in table 2. The fitting of the curves for the grain size and flow behaviour is based on a least-squares approach.

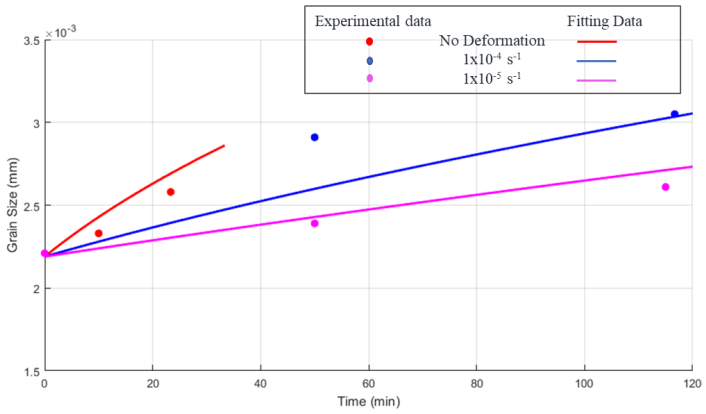

Fig. 7 Fitting of grain size data against time

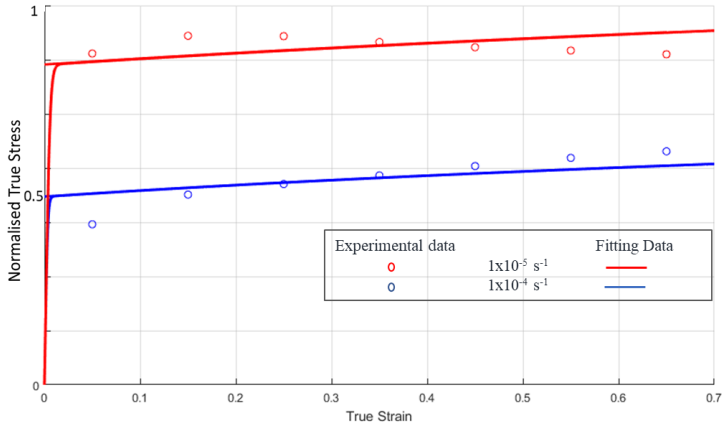

Fig. 8 Fitting of flow stress data against true strain

Table 3 summarises the different conditions used for completing the numerical simulation to obtain the pressure curves for forming trials. Fig. 9 shows the pressure curves from the numerical simulation. Increasing the maximum pressure or decreasing the controlled strain rate leads to longer cycles. At 800 °C, the forming cycle is 61 min at 60 bar and a controlled strain rate of $1x10^{-3}$ s^{-1}. Also, at 800 °C, the forming cycle is 146 min at 30 bar and controlled strain rate of $5x10^{-4}$ s^{-1}. Thus, a reduction of 58% in cycle time can be achieved. Fig. 10 shows the finite element calculations for the grain size and thickness for trial 1. Ti64 sheet materials were cut into blanks of 500 x 500 mm and sprayed with boron nitride for the forming trials. Fig. 11 shows the formed parts. It was noticed that all parts were fully formed.

In terms of pressure cycle prediction, PAMSTAMP software has a more robust methodology in comparison to Abaqus, as a statistical approach is used in order to define the maximum strain-rate over all the integration points of the component at any instant of the forming process. This results in more precise and, as a consequence, shorter pressure cycles. Indeed, very similar pressure cycles have been predicted by both software platforms despite the fact that the targeted strain-rate imposed in Abaqus was 0.001 s^{-1}, twice the targeted strain-rate imposed in PAMSTAMP.

Table 3 Modelling conditions for SPF process

	Condition			
	Maximum Pressure (bar)	Temperature (°C)	Controlled Strain rate (s^{-1})	other
Trial 1	60	800	0.001	Abaqus
Trial 2	30	800	0.001	Abaqus, Ironing
Trial 3	30	800	0.001	Abaqus, No ironing
Trial 4	30	800	0.0005	Abaqus
Trial 5	60	800	0.0005	PAMSTAMP

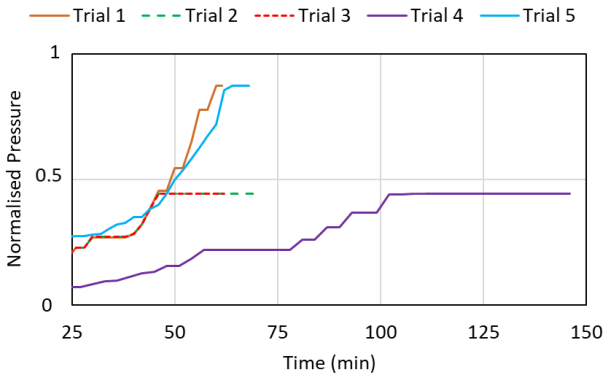

Fig. 9 Pressure curves obtained from numerical simulations

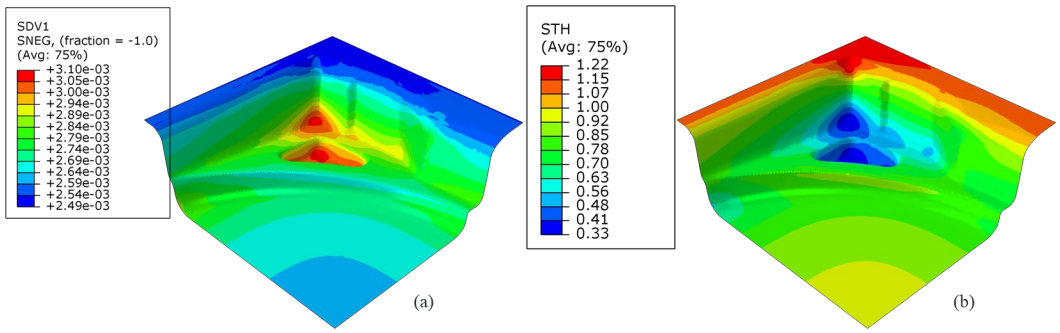

Fig. 10 Finite elements calculations for (a) grain size (mm) and (b) thickness (mm) from trial 1

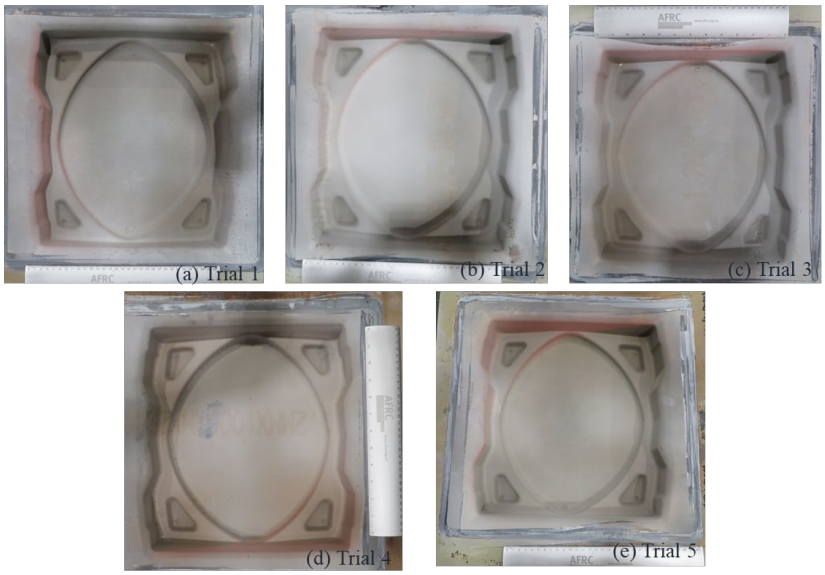

Fig. 11 SPF formed parts (a) trial 1 (b) trial 2 (c) trial 3 (d) trial 4 (e) trial 5

Conclusions

Based on its multiple benefits, potential reductions in the temperature of SPF processes have been analysed in the present work using Ti64 material from TIMET. Experimental and modelling work have shown the possibility of a temperature reduction of at least 100 °C for the component here analysed with respect to traditional SPF forming temperatures. The Ti64 material has been analysed from a mechanical testing and a microstructural point of view. Results from the tensile tests at high temperature show the outstanding behaviour of this material from an SPF point of view, with high values of the strain rate sensitivity (close to 0.6 in many cases), as well as absence of failure for the temperature ranges here analysed (from to 750 °C to 800 °C). The microstructure of the as-received material has proven to be a key aspect to enable the temperature reduction, with an as-received average grain size of 2.3 μm. Absence of cavitation has been verified for the multiple process conditions here analysed. Modelling work using a microstructural model has proven the possibility of forming a complex component shape at the temperatures of interest.

Different components have been formed based on the pressure cycles predicted by the simulation work, validating the modelling as well as the general approach for the temperature reduction. In addition, a time reduction in the pressure cycle has been achieved by the usage of advanced software for SPF simulation.

As it has been shown in this work, the pressure values for any proposed temperature reduction will increase in value, in the present work pressures up to 60 bar would be required (also the tonnage associated to the pressure cycle), as the material develops higher internal stresses in comparison to SPF at conventional temperatures. Any temperature reduction attempt would need

to consider if the pressure and the hydraulic systems of the press will be able to deliver the required pressure and tonnage increments. As the reader can guess, the answer to this question is dependent on the amount of temperature reduction and the component characteristics (overall size, radii of the features, etc.). There could be cases where more powerful systems would be required to be either installed or designed (if the press is in the design stage). A cost analysis would solve for each case if the associated capital expenditure costs were compensated by all the benefits of a lower temperature process: reduction on the energy costs, cheaper material for dies and platens (also an increase in their life), less maintenance costs, longer production shifts and less consumables.

References

[1] R.R. Boyer, An overview on the use of titanium in the aerospace industry, Mater. Sci. Eng. A. 213 (1996) 103-114. https://doi.org/10.1016/0921-5093(96)10233-1

[2] E. Alabort, P. Kontis, D. Barba, K. Dragnevski, R.C. Reed, On the mechanisms of superplasticity in Ti-6Al-4V, Acta Mater. 105 (2016) 449-463. https://doi.org/10.1016/j.actamat.2015.12.003

[3] E. Alabort, D. Putman, R.C. Reed, Superplasticity in Ti-6Al-4V: Characterisation, modelling and applications, Acta Mater. 95 (2015) 428-442. https://doi.org/10.1016/j.actamat.2015.04.056

[4] P. Mandal, A. Gomez-Gallegos, D. Gonzalez, H. Elrakayby, P. Blackwell, Superplastic Behaviour of Ti54M and Ti64, MATEC Web Conf. 321 (2020) 04028. https://doi.org/10.1051/matecconf/202032104028

[5] F. Pitt, M. Ramulu, Influence of grain size and microstructure on oxidation rates in titanium alloy Ti-6Al-4V under superplastic forming conditions, J. Mater. Eng. Perform. 13 (2004) 727-734. https://doi.org/10.1361/10599490421394

[6] G.A. Salishchev, R.M. Galeyev, O.R. Valiakhmetov, R. V. Safiullin, R.Y. Lutfullin, O.N. Senkov, F.H. Froes, O.A. Kaibyshev, Development of Ti-6Al-4V sheet with low temperature superplastic properties, J. Mater. Process. Technol. 116 (2001) 265-268. https://doi.org/10.1016/S0924-0136(01)01037-8

[7] R.S. Mishra, V. V. Stolyarov, C. Echer, R.Z. Valiev, A.K. Mukherjee, Mechanical behavior and superplasticity of a severe plastic deformation processed nanocrystalline Ti-6Al-4V alloy, Mater. Sci. Eng. A. 298 (2001) 44-50. https://doi.org/10.1016/S0921-5093(00)01338-1

[8] H. Matsumoto, K. Yoshida, S.H. Lee, Y. Ono, A. Chiba, Ti-6Al-4V alloy with an ultrafine-grained microstructure exhibiting low-temperature-high-strain-rate superplasticity, Mater. Lett. 98 (2013) 209-212. https://doi.org/10.1016/j.matlet.2013.02.033

[9] J. Lin, T. Zhu, L. Zhan, Constitutive equations for modelling superplastic forming of metals, in: Superplast. Form. Adv. Met. Mater., Elsevier, 2011: pp. 154-183. https://doi.org/10.1533/9780857092779.2.154

[10] T.G. Langdon, Grain boundary sliding revisited: Developments in sliding over four decades, J. Mater. Sci. 41 (2006) 597-609. https://doi.org/10.1007/s10853-006-6476-0

[11] H. Elrakayby, D. Gonzalez, A. Gomez-Gallegos, P. Mandal, N. Zuelli, A Study on Modelling the Superplastic Behaviour of Ti54M Alloy, Solid State Phenom. 306 (2020) 9-14. https://doi.org/10.4028/www.scientific.net/SSP.306.9